Solution chemistry and corrosion

Nils-Gösta Vannerberg

Eka Nobel AB, S-445 01 Surte, Sweden

Abstract - A metallic material is very seldom in chemical
equilibrium with its surroundings; it corrodes. The most im-
portant form of corrosion is the atmospheric one. This is not
a simple oxidation but a complicated electrochemical process
taking place in a liquid interphase covering the solid mate-
rial. It is mostly governed by small amounts of pollutants
like SO_2 and NO_2, and in industrial environment also by Cl_2
and H_2S. In such surroundings even materials covered with gold
corrode forming complexes like $AuCl_4^-$ etc.

The atmospheric degradation of iron and steel costs the soci-
ety enormous sums of money each year. This paper will there-
fore concentrate on sulphur dioxide induced iron corrosion. A
laboratory experiment shows that for each SO_2 molecule adsorb-
ed onto an iron surface, 60 iron atoms are oxidized into cor-
rosion products. The process might be interpreted as an elec-
trochemically governed reaction triggered by SO_2.

The electrochemistry of iron and iron oxides as investigated
by equilibrium studies, potentiodynamic studies both in active
and in passive states, impedance measurements, and ESCA will
be discussed. Finally a semi-quantative mechanism for the cor-
rosion is given. SO_2 breaks the passivation of the iron sur-
face and, iron ions leave the surface until oxygen passivates
it again.

INTRODUCTION

Corrosion is Greek for "gnawing". An agent gnaws away at a solid material,
most often a construction metal. This "gnawing agent" is most often a solu-
tion and it is the properties of this solution which determine the type of
corrosion.

Between the solid phase and the solution phase there is a zone, called an
interphase. It is the properties of this interphase which will be the focus
of this paper.

CORROSION AND EQUILIBRIUM

For a long time the so-called Pourbaix diagram has been an important tool
in determining the ultimate state not only in a corroding system but, on the
whole, in inorganic chemistry.

In a two-dimensional diagram, Fig. 1.a, the ordinate represents the redox po-
tential while the abscissa represents the pH. The different fields as shown
in the diagram represent areas where a defined species dominates. It is of
course possible to let a third and a fourth axis represent the concentration
of different ligands but this is seldom done for obvious practical reasons.
Instead a fixed molar relation between two elements is prescribed.

Figure 1.b exhibits another type of diagram. The logarithm of the relative
activities is plotted against the pe or redox potential. At high redox poten-
tial and in acidic solution, copper is oxidized into copper(II) ions. At low
potentials copper(I) sulphide is formed. Copper between these two potentials
is thermodynamically stable. This diagram has been the basis for the Swedish
solution to the problem of nuclear waste(ref.1). The nuclear waste is stored in
copper canisters, which are surrounded by a redox buffer with a redox poten-
tial of -100 mV. At this potential the copper metal is thermodynamically
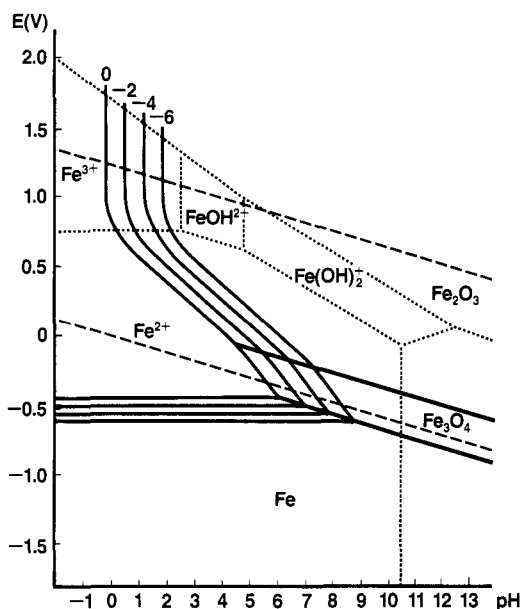stable.

Fig. 1.a. Pourbaix diagram for the
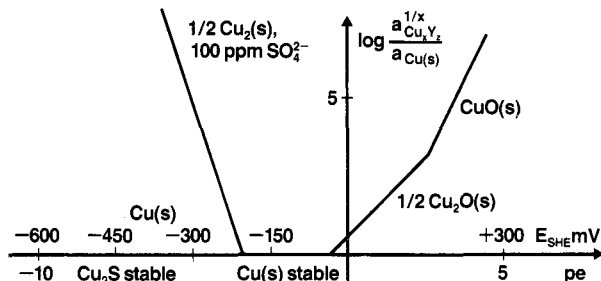iron and water system at 25°C.

Fig. 1.b. Redox diagram for the system
$Cu-H_2O-Cl^--CO_3^{2-}-SO_4^{2-}-F^-$
at 25°C, pH=8.5 (ordinary water).

ATMOSPHERIC CORROSION

The Pourbaix diagram is most valuable in identifying the state of equilibrium.
However, a corroding system is never in equilibrium or even close to equi-
librium. In fact, the kinetics of the corrosion process is generally of much
more value than the ultimate state. This paper will concentrate on the de-
scription of just one type of corrosion, namely atmospheric corrosion. One may
consider this to be a vain attempt as the title of this paper is: "Solution
chemistry and corrosion".

Actually, atmospheric corrosion always occurs when a liquid phase is adsorbed
onto a metal or onto corrosive products. In the absence of water vapour pres-
sure, i.e. at low humidity, no corrosion or a very slow corrosion can be per-
ceived. Atmospheric corrosion is not a simple oxidation. In fact, it is con-
trolled by small amounts of air pollutants such as sulphur dioxide, nitrogen
oxide etc.

The adsorption of radioactive sulphur dioxide onto the most important con-
struction metals - iron, zinc, copper, and aluminium - has been measured as a
function of time. Depending on the pretreatment of the samples all of them
were covered by a very thin oxide film, Fig. 2 (ref. 2).

Aluminium metal adsorbs sulphur dioxide onto its surface to a small extent.
Moreover the adsorption terminates when the surface is covered by a one-
molecular thick layer of sulphur dioxide molecules. Sulphur dioxide is ad-
sorbed onto zinc and copper in quite a different way. The adsorption follows
a parabolic rate law. Such a rate law is found when the corrosion products
form a diffusion barrier between the metal and the corrosive solution. The
thicker the barrier, the slower the reaction. It can easily be shown that the
corrosion products contain a little more than one metal ion per sulphur atom;
in fact they consist of basic sulphates.

The adsorption of sulphur dioxide onto iron is less trivial. As can be seen,
it goes through an induction period but accelerates then up to a constant
value, Fig. 3. It is the gas phase limited diffusion which determines the ad-
sorption rate.

Moreover the corrosion products are not sulphates but iron oxide hydroxide,
FeOOH(s), Fig. 4,(ref. 3). It can be shown that about sixty iron atoms are
oxidized due to the adsorption of one single sulphur dioxide molecule. As-
suming relevant deposition velocities, the corrosion in laboratory and field
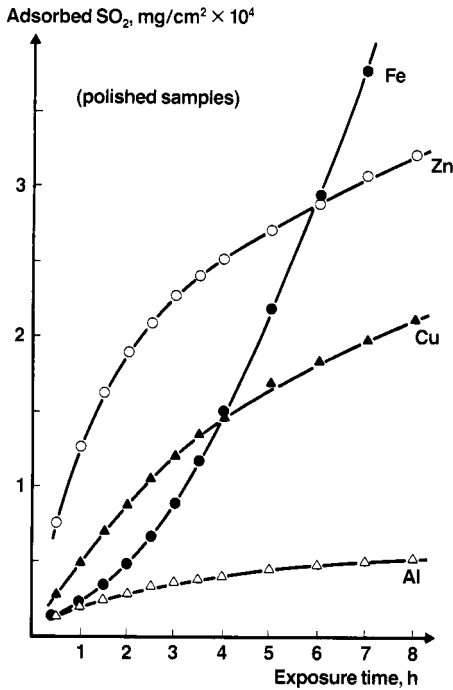tests can be compared. As is evident, the results agree well, Table 1 (ref. 4).

Adsorbed SO$_2$, mg/cm^2 × 10^4

(polished samples)

Fe

Zn

Cu

Al

Exposure time, h

Fig. 2. Adsorption of sulphur dioxide onto polished metal samples as a function of time; relative humidity 90%.

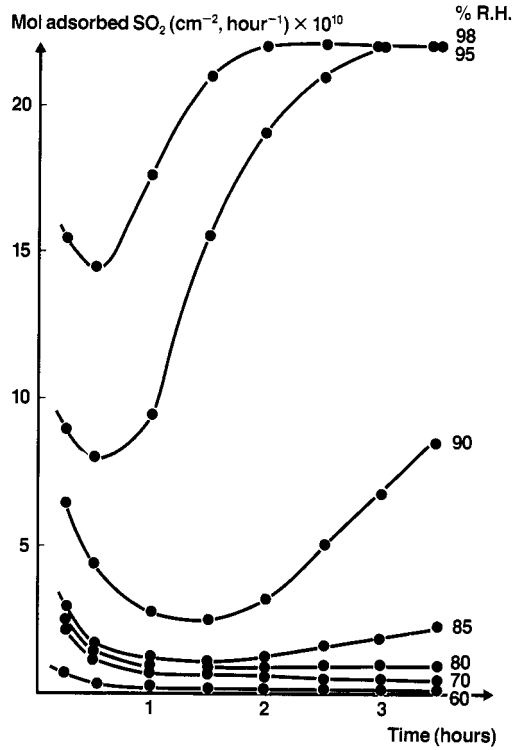Mol adsorbed SO$_2$ (cm^{-2}, hour^{-1}) × 10^{10} % R.H.

98
95

90

85

80
70
60

Time (hours)

Fig. 3. Adsorption rate of sulphur dioxide onto polished samples of iron as a function of time and relative humidity.

W (mg cm^{-2})

SO$_2$-supply
(μg · cm^{-2} · h^{-1})
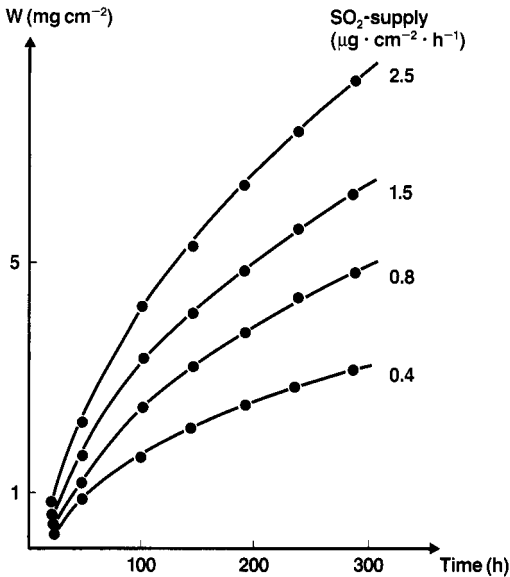
2.5

1.5

0.8

0.4

Time (h)

Fig. 4. Weight increase of steel samples exposed to 1 ppm SO$_2$ at different flow rates. SO$_2$ supplies are given in the figure. Relative humidity was 96% and the temperature was 22.0°C.

TABLE 1. Comparison between laboratory and outdoor atmospheric corrosion of carbon steel.

Exp.	Corrosion in laboratory experiments expressed as metal loss per month (g Fe m^{-2} month^{-1})	Calculated corrosion rates from our modified version of Haagenrud's correlation (g Fe m^{-2} month^{-1})
1	44	62
2	71	92
3	78	169
4	128	156
5	196	327

Gold is nowadays a common contact material used i.e. as electrical switches in computers. However, in an industrial environment even gold corrodes. In atmospheres containing small amounts of NO_2, SO_2, Cl_2, and SO_2, gold catalyzes the formation of sulphuric acid, which is detrimental to other materials, but not to the gold itself, Fig. 5 (ref. 5).
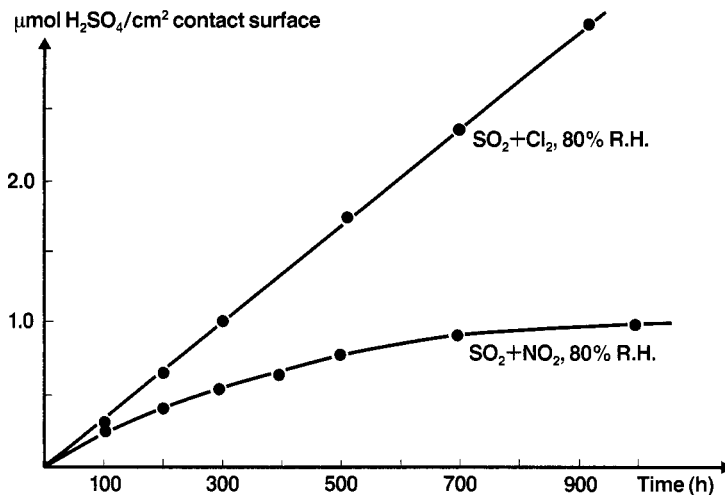

Fig. 5.   Formation of H_2SO_4 on a gold surface.

However, in a surrounding contaminated by small amounts of NO_2 and Cl_2 gold is oxidized into tetrachloroauric acid, which precipitates onto the gold surface, Fig. 6.

IRON AND IRON OXIDE ELECTRODES

The unusual stoichiometric relationship $1SO_2$ <—> $60Fe$ show that the sulphur dioxide induced corrosion of iron is of electrochemical origin. Iron in an oxygenated environment is always covered by an oxide film. It can thus be worthwhile not only to study the iron metal but also the iron oxide as an electrode.

Still the most efficient way to study electrode kinetics is the potentiodynamic method. Three electrodes are used: a working electrode consisting of the material you wish to study; a measuring electrode by which the electrode potential is measured at the surface of the working electrode; and a counter electrode. The current passing through the system, through the working and the counter electrodes is measured, Fig. 7.
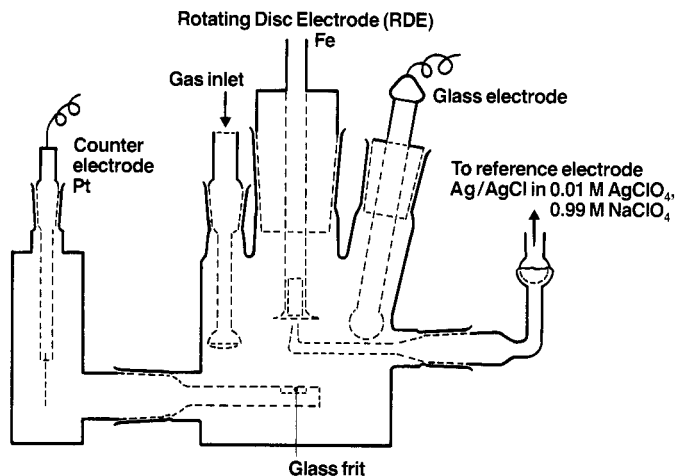

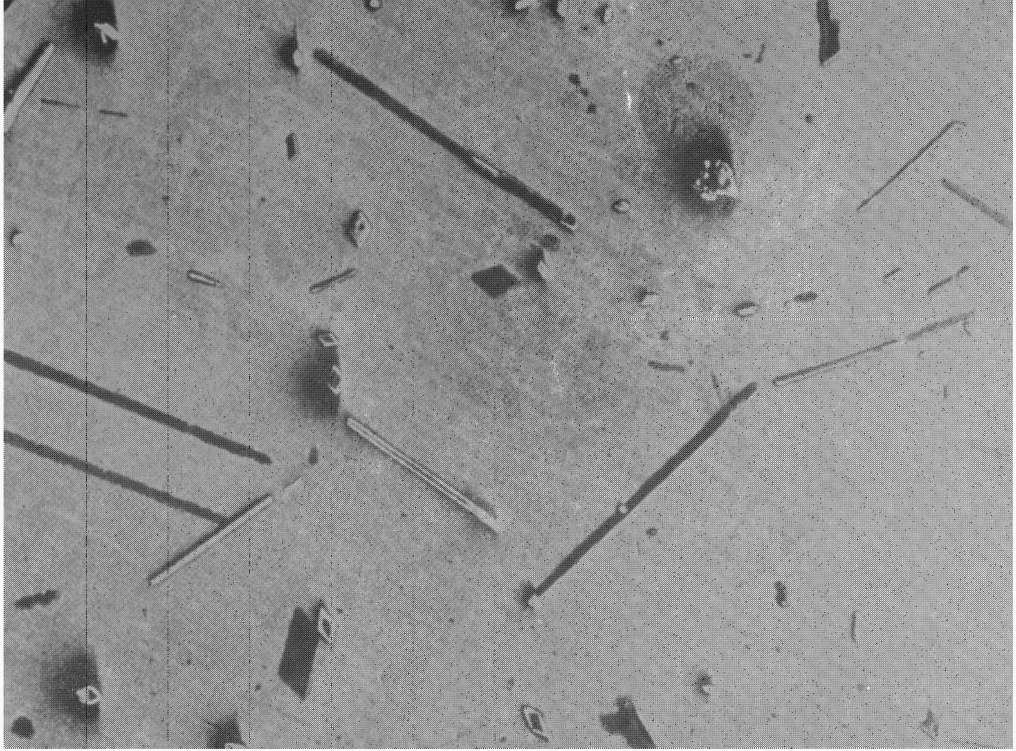Fig. 7.   Cell for rotating disc electrodes.

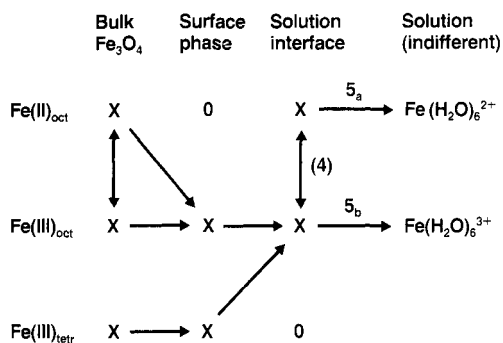Fig. 6. Pure gold exposed to 500 h in 0.05 ppm Cl_2 + 0.5 ppm NO_2, 80% relative humidity, enlargement 60 x.
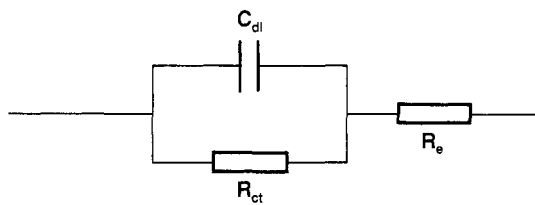
Bulk Fe_3O_4	Surface phase	Solution interface	Solution (indifferent)

Fe(II)$_{oct}$ X   0   X $\xrightarrow{\ 5_a\ }$ Fe$(H_2O)_6^{2+}$

$\Big\updownarrow$ $\searrow$ $\Big\updownarrow$ (4)

Fe(III)$_{oct}$ X $\longrightarrow$ X $\longrightarrow$ X $\xrightarrow{\ 5_b\ }$ Fe$(H_2O)_6^{3+}$

$\nearrow$

Fe(III)$_{tetr}$ X $\longrightarrow$ X   0

C_{dl} = double layer capacitance
R_{ct} = charge transfer resistance
R_e = electrolyte resistance

Fig. 8. Dissolution paths of mag-   Fig. 9. Equivalent circuit.
netite in acid media in the region
of its free potential.

From plots of the current or the logarithm of the current versus the measured
potential at the working electrode, the mechanism of the kinetics of the elec-
trode process can be evaluated, Fig. 8 (refs. 5,6,9).

The connection between the current and the electrode potential quite often
follows the Butler-Volmer equation:

$$i = i_0 ([A^{z+}] \cdot e^{\eta / \frac{RT}{\alpha F}} - [A] \cdot e^{-\eta / \frac{RT}{(1-\alpha)F}})$$

For a material not far from the equilibrium or corrosion potential, the equa-
tion can be written as a Tafel equation:

$$\log i = \frac{\eta}{b} + a$$

When the potential between the electrode and the solution is changed, the
electrode will be charged at the same time as the current is flowing. In a
way it is the problem of a leaking condensator, Fig. 9.

Measurements of the impedance can give valuable information about the pro-
cesses taking place in the interphase. However, the data is generally hard
to interpret.

Direct spectroscopic evidence about species in the interphase is difficult to
find. Elipsometric measurements are possible as well as enhanced Raman
spectroscopy. Sometimes ESCA measurements of the dried electrode surfaces can
produce interesting results.

Figure 10 exhibits the connection between the current density and the elec-
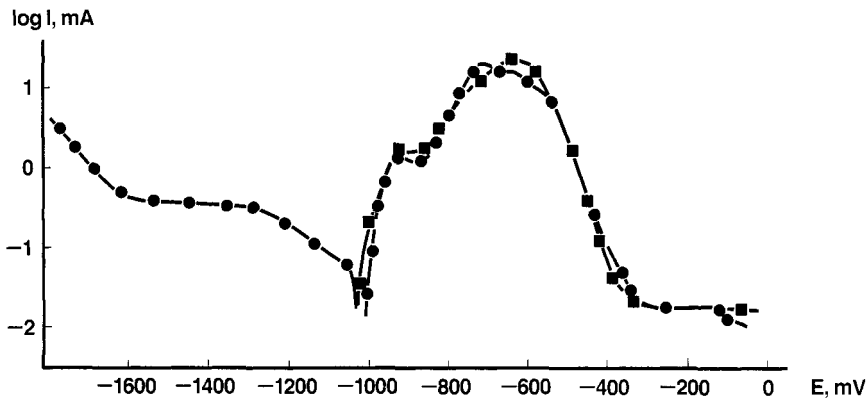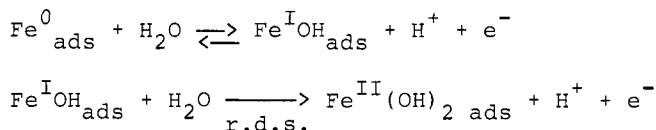trode potential for an iron electrode pre-etched in the solution (ref. 6).

Fig. 10. Polarization curve for pure iron in 1 M(Na+H)ClO$_4$
for pH=3. The experimental curve (●) is compared with
theoretically calculated curve (■) for anodic dissolution.

As an anode, the electrode behaves somewhat specific. Near the corrosion potential there is a current density with a Tafel slope of 40 mV and a pH dependance of 1, i.e.

$$\log i = \frac{\eta}{40} + pH + constant$$

This state is called I_1, which fits the following stoichiometric mechanism:

$$Fe^0_{ads} + H_2O \underset{\longleftarrow}{\overset{\longrightarrow}{}} Fe^I OH_{ads} + H^+ + e^-$$

$$Fe^I OH_{ads} + H_2O \xrightarrow[r.d.s.]{} Fe^{II}(OH)_{2\ ads} + H^+ + e^-$$

This reaction takes place most certainly at defects on the iron surface. When the defects are covered by adsorbed Fe(OH)$_2$ species, another reaction takes place. This reaction has a Tafel slope of 120 mV and is not dependent upon the pH value.

$$\log i = \frac{\eta}{120} + constant$$

This state is called I_2. There is much controversy about the origin of this reaction.

For the time being it might be assumed that the reaction

$$Fe^0_{surf} + H_2O \xrightarrow[r.d.s.]{} Fe^I OH_{ads} + H^+ + e^-$$
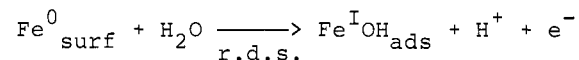
is the rate-determining step.

At high potentials the current density decreases and one ends up with a potentially independent state. This behaviour will be discussed in connection with the magnetite electrode.

An iron electrode, which is left at the corrosion potential to corrode for an hour or more, shows a completely different behaviour (7). In the so-called I_1^- state the current potential relation is

$$\log i = \frac{\eta}{120-160} + constant$$

As is evident from experiments given below, in the I_1^- state the iron electrode is covered by an oxide layer. If the electrode potential is increased, it suddenly changes from the I_1^- state into the I_2 state, Fig. 11. The I_1^- state is encouraged by the presence of a soft Lewis base such as I$^-$, CN$^-$, and H$_2$C$_2$.

An ESCA investigation shows that the electrode in the I_1^- state is covered by a 5 nm thick iron oxide film. If the behaviour is aggravated by iodide ions these are in turn incorporated. The corresponding I_2 state film is very thin, contains no iodine and is probably formed in the air when handling the electrode, Fig.12 (ref. 8).

In the cathodic range, Fig. 13, at a low pH value, the results are rather easy to interpret. Over the whole range of potentials, the following stoichiometric mechanism seems to determine the reaction rate.

$$H^+ + e^- \underset{\longleftarrow}{\overset{\longrightarrow}{}} H_{ads} \qquad H_{ads} + H^+ + e^- \xrightarrow[r.d.s.]{} H_2(g)$$
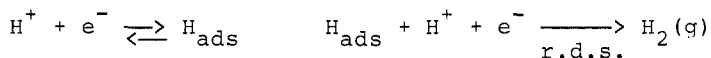
This is the Heyrovsky mechanism. (7)

There is a pH dependence of -2 and a Tafel slope of -40 mV near the corrosion potential; and a pH dependence of -1 and a Tafel slope of -120 mV when the H$_{ads}$ alone, cover the surface completely. At low potentials the reaction has a pH dependence of -1 and is potentially independent. This means that the
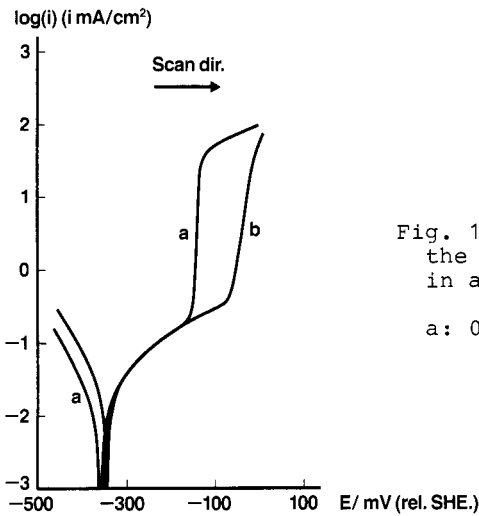
Fig. 11. The effect of sweep rate on the polarization diagram for iron in a saturated acetylene solution.

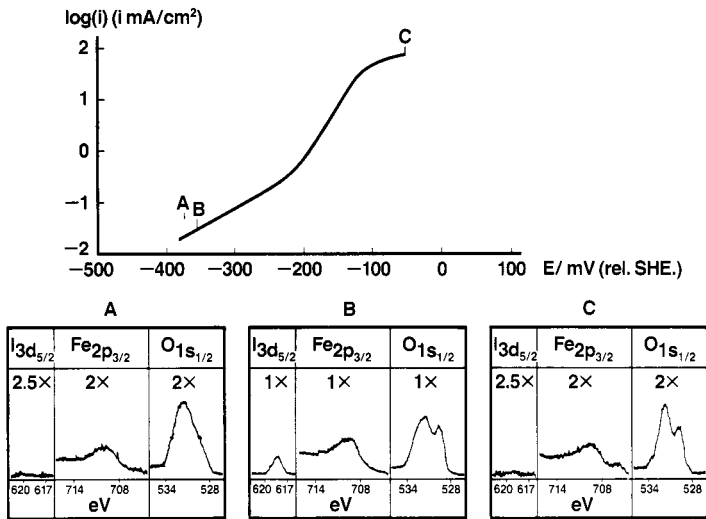a: 0.5 mV/s, pH=2   b: 5 mV/s, pH=2

Fig. 12. The polarization diagram in presence of 45 mM I^-. ESCA measurements of O, Fe and I^- for the different electrode states.

Current density as function of the electrode potential

Iron electrode 0.999 M $NaClO_4$
0.001 M $HClO_4$

Gradient decade / 0.118

$2H^+ + 2e^- \longrightarrow H_2$
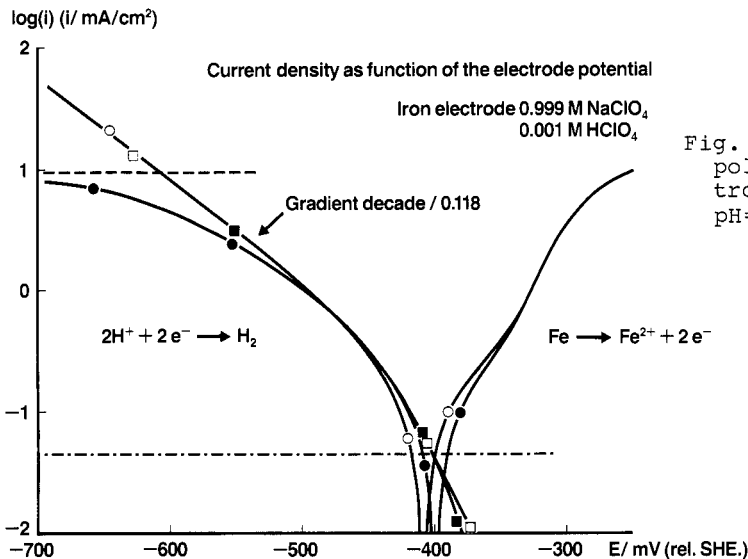
$Fe \longrightarrow Fe^{2+} + 2e^-$

Fig. 13. Anodic and cathodic polarization of an iron electrode in 1.00 M(Na+H)ClO_4 for pH=3.00.
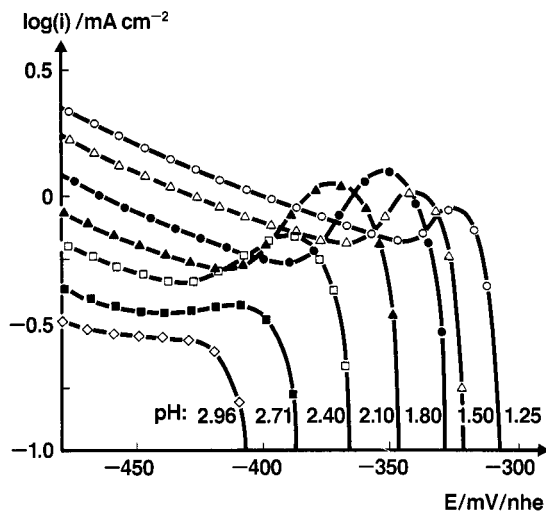
Fig. 14.a. Cathodic-going potential
  sweeps started from anodic poten-
  tials (the anodic branches starting
  ca. 250 mV more anodic than the cor-
  rosion potential are not shown). The
  electrode starts in state A, but is
  transformed into state B during the
  anodic part of the sweep.
  1.00 M(Na+H)ClO$_4$, pH as indicated on
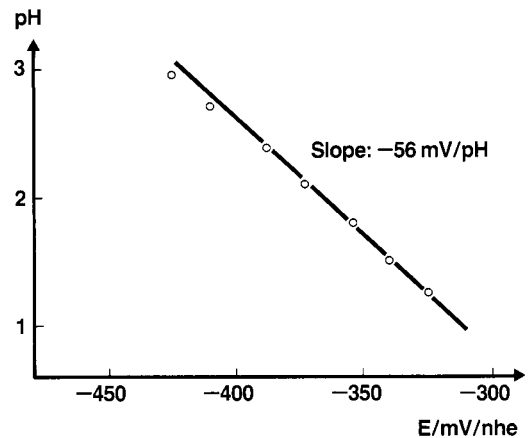 the sweep curves, 27°C, 50 rps,
  5 mVs^{-1}.

Fig. 14.b. Plot of peak-potentials
  from Fig. 14.a vs pH.

diffusion of hydrogen ions onto the surface determines the reaction rate. At
all potentials there is a small contribution to the current from the reaction

$$2H_{ads} \longrightarrow H_2.$$

If an iron electrode has been polarised into the I_2 region and then is used
as a cathode, there appears to be a reduction of some kind of a magnetite-like
species, Fig. 14.a and 14.b (ref. 9).

In order to understand the behaviour of the iron electrode in a passive state,
i.e. at high redox potentials, it is advantageous to study the magnetite elec-
trode. It is very easy to grow single crystals out of the material. Moreover,
in the passive iron metal system there are probably three different phases of
iron: iron itself, a magnetite-like phase, and probably some maghemite phase
(γ-Fe$_2$O$_3$), which could be Fe$_5$HO$_8$. In the case of magnetite, there are one pha-
se and one interphase which can both be easily controlled and defined (ref. 10).

The current potential diagram of the magnetite electrode is remarkably similar
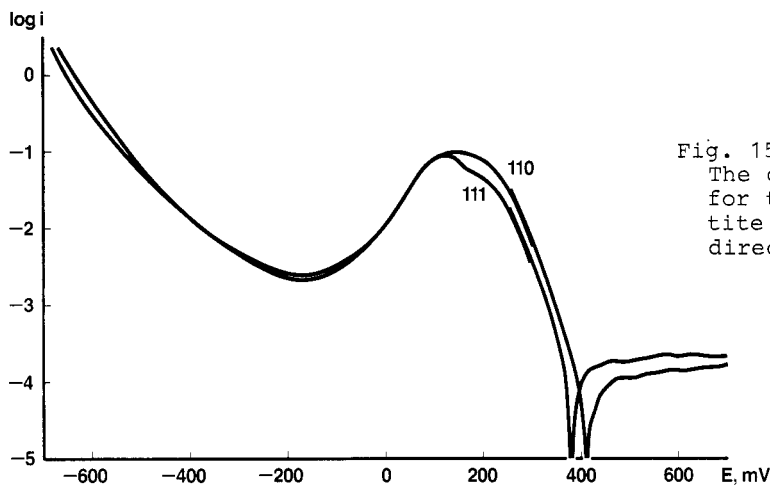to the corresponding iron electrode diagram, Fig. 15.

Fig. 15.
  The current potential diagram
  for the single crystal magne-
  tite electrode, 110 and 111
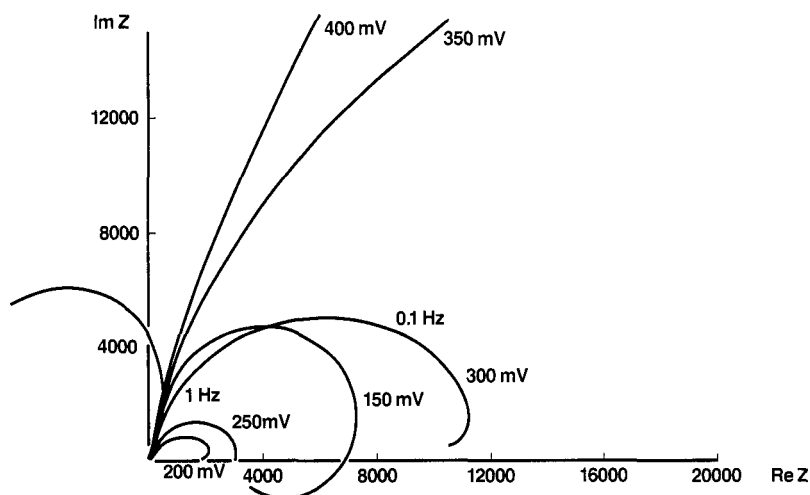 directions (ref. 10).

Fig. 16. The impedence of a magnetite electrode at different potentials (ref. 10).

A closer look at the high potential region shows a clear passive region and on the cathodic side a rise in the current when decreasing the potential. The Tafel slope is 60 mV here and the pH behaviour -1.5.

$$\log /i/ = \frac{n}{60} - 1.5\ pH$$

The impedance measurement shows reactions of slow rate at high potentials and rapid rate at low potentials, Fig. 16. The reactions can be described in the following way. At high potentials the dissolution of magnetite follows the reaction:

$$Fe_3O_4 + 8H^+ \longrightarrow 3Fe^{3+}(aq) + 8H_2O + e^- \tag{1}$$
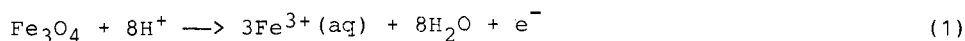
This is a very slow overall reaction.

At low potentials the dissolution reaction is:

$$Fe_3O_4 + 8H^+ + 2e^- \longrightarrow 3Fe^{2+}(aq) + 8H_2O \tag{2}$$
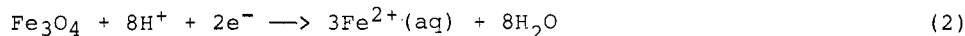
This is a rapid reaction. It is easy to show by analytical methods that these are the two reactions which really take place (ref.9).In the area of the cathodic rise it is only reaction 2 which takes place. The mechanism can be explained in the following way. In the interphase, Fig. 8, the equilibrium

$$Fe(II)_{oct}-OH_2 \rightleftarrows Fe(III)_{oct}-OH + H^+ + e^- \tag{3}$$
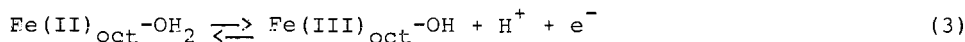
is determined by the redox potential pressed upon the system and the pH of the solution. The reaction 3 has to take place three times in order to complete reaction 2, which explains the odd pH dependence of 1.5.

In the whole cathodic rise, the interphase consists almost exclusively of Fe(III) groups. The reactivity of the Fe(II) groups is, however, such that only this species leaves the surface.

MECHANISM FOR ATMOSPHERIC CORROSION ON IRON

An iron surface is completely covered by an oxide layer, in which the outer-most layers only consist of the iron(III) species. The corrosion due to oxygen oxidation is slow, as the reaction Fe (covered with iron oxide) $\longrightarrow$ Fe^{3+}(aq) +3e$^-$ takes place. The oxygen reduction is coupled to the oxidizing of iron and is then slow. The redox potential of the surface is ill-defined. As is evident, there is an incubation period before the sulphur dioxide induced corrosion starts. When started, the corrosion rate increases several powers of 10. The reaction rates are controlled by the activation of electrochemically active sites due to the sulphur dioxide molecules and the passivation of the same sites by oxygen.

REFERENCES

1. Koppar som kapslingsmaterial för icke upparbetat kärnbränsleavfall. Bedöm-
   ning ur korrosionssynpunkt. KBS Teknisk Rapport 90 (1978)
2. T. Sydberger and N.-G. Vannerberg, Corrosion Science 12, 775 (1972)
3. T. Sydberger and R. Ericsson, Werkst. Korros. 28, 154 (1977)
4. L.-G. Johansson: SO_2-induced corrosion of carbon steel in various atmo-
   spheres and dew point corrosion in stack gases, Dept. Inorg. Chem.,
   University of Göteborg and Chalmers University of Technology, Sweden (1982)
5. O. Svedung: The influence of different corrosive mixed-gas atmospheres on
   gold-coated materials, Dept. Inorg. Chem., University of Göteborg and
   Chalmers University of Technology, Sweden (1986)
6. P. Nilsson: The kinetics of the iron electrode in acid solutions, Dept.
   Inorg. Chem., University of Göteborg and Chalmers University of Technology,
   Sweden (1979)
7. B. Håkansson: The corrosion of iron in acid solution, Dept. Inorg. Chem.,
   University of Göteborg and Chalmers University of Technology, Sweden (1982)
8. E. Ahlberg, G. Ström and N.-G. Vannerberg: An alternative reaction path for
   the dissolution of iron in acid solution, 9th Scandinavian Corrosion Con-
   gress
9. B. Håkansson, N.-G. Vannerberg, and G. Bech-Nielsen, Electrochimica Acta 28,
   451 (1983)
10. M. Ström and N.-G. Vannerberg, to be published.